Instantons for the Destabilization of the Inner Solar System

Eric Woillez[1,2] and Freddy Bouchet[1]

[1]*Université Lyon, Ens de Lyon, Univ Claude Bernard, CNRS, Laboratoire de Physique, F-69342 Lyon, France*
[2]*Department of Physics, Technion, Haifa 32000, Israel*

For rare events, path probabilities often concentrate close to a predictable path, called instanton. First developed in statistical physics and field theory, instantons are action minimizers in a path integral representation. For chaotic deterministic systems, where no such action is known, shall we expect path probabilities to concentrate close to an instanton? We address this question for the dynamics of the terrestrial bodies of the Solar System. It is known that the destabilization of the inner Solar System might occur with a low probability, within a few hundred million years, or billion years, through a resonance between the motions of Mercury and Jupiter perihelia. In a simple deterministic model of Mercury dynamics, we show that the first exit time of such a resonance can be computed. We predict the related instanton and demonstrate that path probabilities actually concentrate close to this instanton, for events which occur within a few hundred million years. We discuss the possible implications for the actual Solar System.

Rare events can be very important if their large impact compensate for their low probability. From a dynamical perspective, when conditioned on the occurrence of a rare event, path probabilities often concentrate close to a predictable path, called instanton. This is a key and fascinating property for the dynamics of rare events and of their impact [1], which was first observed in statistical physics, for the nucleation of a classical supersaturated vapor [2]. Soon after, a similar concentration of path probabilities has been studied in gauge field theories [3,4], for instance for the Yang-Mill theory. Instantons continue to have a number of applications in modern statistical physics, for instance to describe excitation chains at the glass transition [5], reaction paths in chemistry [6], escape of Brownian particles in soft matter [7], MHD [8] and turbulence [9–13], among many other examples. Moreover, a large effort has been pursued to develop dedicated numerical approaches to compute instantons [14]. Inspired by the earlier works, action minimization has found a rigorous mathematical treatment through the Freidlin-Wentzell large deviation theory [15] of ordinary differential equations with small noises [16].

In all those classical or quantum applications, instantons appear as action minimizers, for a saddle point evaluation of a path integral. The basic property of the instanton phenomenology is that, conditioned on the occurrence of a rare event, path probabilities concentrate close to a predictable path. Figure 1 gives an illustration of this property for a particle in a bistable potential. Shall we expect this phenomenology to be valid for systems for which the Freidlin-Wentzell action [17] does not exist in the first place, for instance chaotic deterministic systems? The main

aim of this Letter is to open this fascinating question for a paradigmatic problem in the history of physics: the dynamics of the Solar System. Shall we expect an instanton phenomenology for rare events that shaped or will shape the Solar System history?

The discovery that our solar system is chaotic with a Lyapunov time of about five million years [18–20] has disproved the previous belief that planetary motion would be predictable with any desired degree of precision. On the contrary, chaotic motion sets an horizon of predictability of a few tens of millions of years for the solar system. Even more striking has been the discovery that about 1% of the trajectories in the Solar System lead to collisions between planets, or between planets and the Sun within five billion
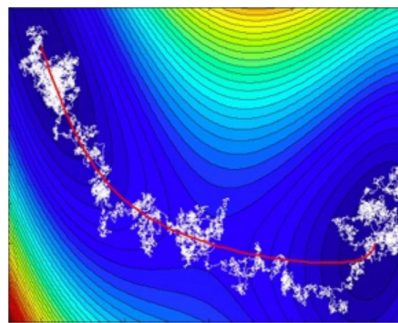
FIG. 1. Instanton for a Brownian particle in a bistable potential. The particle's trajectory from one attractor to another (white line) closely follows the minimum action path (instanton, red line), up to thermal fluctuations. The level curves of the potential are displayed in the background, with the color scale giving the potential's height (courtesy Eric Vanden-Eijnden).

years [21]. As shown numerically, chaotic disintegration of the inner solar system (i.e., the four terrestrial planets) always happens through a resonance between the motion of Mercury's and Jupiter's perihelia [21–24], related to a large increase in Mercury's eccentricity. Stochastic perturbation to planetary motion exists, for instance through the chaotic motion of the asteroid belt, but is too weak to be responsible for the rare destabilizations of the inner solar system [23,25]. Instead, stochasticity in the solar system appears because of the development of internal deterministic chaos [23].

Does an instanton phenomenology exist for the rare destabilization of the Solar System? Our first result will be obtained within a simplified model of Mercury's dynamics [26]. We predict for this model the probability distribution of the first destabilization time, the instanton paths, and check the instanton phenomenology.

The secular dynamics describes the planetary motion averaged over fast orbital motion. The secular dynamics Hamiltonian is

$$H(\mathbf{I}, \mathbf{\Phi}) = H_{\text{int}}(\mathbf{I}) + \sum_{\mathbf{k} \in \mathbb{Z}^{16}} A^k(\mathbf{I}) \cos(\mathbf{k}.\mathbf{\Phi}), \quad (1)$$

where $(\mathbf{I}, \mathbf{\Phi})$ is the canonical set of Poincaré action-angle variables for the eight planets, $\mathbf{k}$ is a vector of integers, and the coefficients A^k are functions of the action variables only (see, e.g., [27] for the explicit expression of H to forth order in planetary eccentricities and inclinations). We will study Mercury's possible destabilization in the framework of a simplified model proposed by Batygin *et al.* [26]. This model should be seen as a minimal model retaining the relevant interactions leading to destabilization of the inner Solar System but is not expected to describe quantitatively the inner Solar System.

The approximations of [26] consist in keeping only the degrees of freedom of a massless Mercury in the Hamiltonian (1), and replace all other action-angle variables by their quasiperiodic approximation. Assuming moreover that only a small number of periodic terms in Eq. (1) significantly affect the long-term secular motion of Mercury [22,24, 26,28], Mercury's simplified Hamiltonian is

$$H = H_{\text{int}}(I, J) + E_2\sqrt{I}\cos(\varphi) + S_2\sqrt{J}\cos(\psi)$$
$$+ E_T\sqrt{I}\cos[\varphi + (g_2 - g_5)t + \beta], \quad (2)$$

where φ and ψ are the canonical angles conjugated to $I = 1 - \sqrt{1-e^2}$ and $J = \sqrt{1-e^2}(1 - \cos i)$, respectively, and e and i are Mercury's eccentricity and inclination [26]. g_5, g_2, and s_2 are frequencies involved in the quasiperiodic decomposition of the motion of Jupiter (g_5) and Venus (g_2 and s_2). The numerical values for the other coefficients in Eq. (2) are given in [29].

A slow variable for Mercury's dynamics.—We first show how a slow variable can be built from the dynamics defined

by the Hamiltonian (2). In Eq. (2), H_{int} only depends on the actions. Would the total Hamiltonian be reduced to this part, the actions would be constant and the canonical angles would simply grow linearly with time according to Hamilton's equations

$$\dot{\varphi}(t) = \frac{\partial H_{\text{int}}}{\partial I} = -g_1(I, J) + g_5,$$
$$\dot{\psi}(t) = \frac{\partial H_{\text{int}}}{\partial J} = -s_1(I, J) + s_2. \quad (3)$$

The fundamental frequencies $g_1(I, J)$ and $s_1(I, J)$ describe Mercury's perihelion precession at frequency g_1, and its orbital plane oscillations with respect to the invariant reference plane, at frequency s_1. For the model (2), g_1 value is about $5.7''/\text{yr}$, corresponding to a period of about 227000 years [32].

Through the chaotic dynamics of (2), the fundamental frequencies $\{g_1, s_1\}$ change over time. Mercury's secular motion might enter into resonance with the external periodic forcing if g_1 or s_1 comes close to one of the frequencies g_5, g_2, or s_2. In particular, the Mercury-Jupiter perihelion resonance, between g_1 and g_5, might trigger Mercury's destabilization [21–24]. The three curves of equations $g_1(I, J) = g_5$, $s_1(I, J) = s_2$, and $g_1(I, J) = g_2$ can be represented in the (I, J) plane, together with the current values of Mercury's action variables. We obtain in Fig. 2 the so-called resonance map that is now widely used for weakly nonintegrable systems [33,34]. We write (2) as $H = \tilde{H} + H_{\text{pert}}$, with

$$\tilde{H} = H_{\text{int}} + E_2\sqrt{I}\cos(\varphi) + S_2\sqrt{J}\cos(\psi), \quad (4)$$

$$H_{\text{pert}} = E_T\sqrt{I}\cos[\varphi + (g_2 - g_5)t + \beta]. \quad (5)$$

The term H_{pert} given by (5) creates a weak perturbation for Mercury's long-term evolution. To find the order of
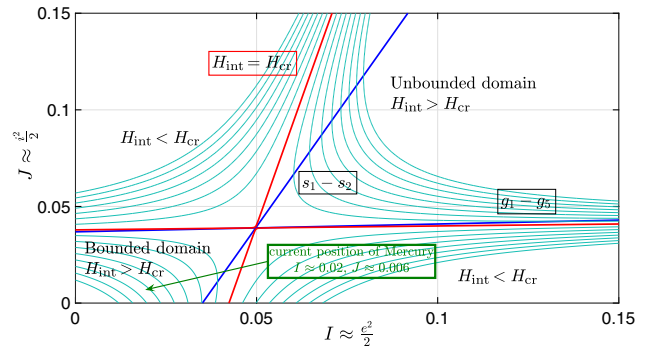
FIG. 2. Level curves of $H_{\text{int}}(I, J)$ in action space. The surface defined by $H_{\text{int}}(I, J)$ has the structure of a saddle. Mercury currently satisfies $H_{\text{int}} > H_{\text{cr}}$ and is located in the bounded domain. For destabilization to occur, Mercury has to cross the saddle and enter the unbounded domain.

magnitude at which H_{pert} affects the long-term dynamics of Mercury, we employ Lie transform methods [34] with the software TRIP [35].

There exists new action-angle variables and a canonical transformation such that Mercury's Hamiltonian can be put in the form

$$H' = \tilde{H}'(I', J', \varphi', \psi') + H'_{\text{pert}}[I', J', \varphi', \psi', (g_2 - g_5)t], \quad (6)$$

where the order of magnitude of H'_{pert} is much smaller than H_{pert}. The Lie transform creates periodic terms in H'_{pert} that contain new combinations of the angles φ', ψ', and $(g_2 - g_5)t$ (given in the Supplemental Material [29]). The difference between H_{pert} and H'_{pert} is that the angular terms of the latter are resonant, which means that their frequencies can vanish. The existence of such resonant terms, even of small amplitude, generate long-term chaotic motion.

The Hamiltonian (6) defines a dynamical system with two well-separated timescales. On a timescale of the order of $(1/g_1)$, the action-angle variables evolve according to Hamilton's equations of motion. The flow is chaotic with a Lyapunov time τ_L of the order of one million years [26]. $\tilde{H}'$ evolution

$$\dot{\tilde{H}}' = \{H'_{\text{pert}}, \tilde{H}'\}, \quad (7)$$

sets a new timescale. In Eq. (7), the notation $\{\}$ represents the canonical Poisson brackets. Equation (7) shows that $\tilde{H}'$ is a slow variable, because its time evolution is driven by $H'_{\text{pert}} \ll H_{\text{pert}}$. As will become clear in the following, $\tilde{H}'$ remains almost constant on the fast timescale, and has only significant variations on a timescale of a few hundred million years.

Diffusion of the slow variable.—The theory of white noise limit for slow-fast dynamical systems (see, e.g., [36]) suggests that on a timescale much larger than τ_L, Eq. (7) is equivalent to a diffusion process. This limit is valid assuming that the variations of $\tilde{H}'$ on the timescale τ_L are sufficiently small. Two additional phenomenological approximations can be made: first, numerical simulations performed with Eq. (7) show that the drift is very small compared to the diffusion coefficient, and can be neglected. Second, the range of $\tilde{H}'$ values before destabilization is small, and the diffusion coefficient can be considered as constant. The long-term evolution of $\tilde{H}'$ can thus be modeled by the standard Brownian motion

$$\dot{\tilde{H}}' = \sqrt{D}\xi(t), \quad (8)$$

where $\xi(t)$ is the Gaussian white noise with correlation function $\langle \xi(t)\xi(t') \rangle = \delta(t - t')$. Unfortunately, the exact expression for D involves the full correlation function of the Hamiltonian flow defined by $\tilde{H}'$. It is too intricate to be useful in practice. Starting from the formal expression, it is shown in the Supplemental Material [29] that an order of magnitude is

$$D \approx 2|H_{\text{pert}}|^6 \tau_L / |\tilde{H}|^4, \quad (9)$$

where $|\tilde{H}|$ and $|H_{\text{pert}}|$ are orders of magnitude of (5) and (4), respectively. Equation (9) is our first important result. Evaluating Eq. (9) gives $D \approx 7.2 \times 10^{-7}$ Myr^{-3}. The associated diffusion timescale for $\tilde{H}'$ is evaluated to one billion years. Those results justifies the self-consistency of the choice for the slow variable.

Distribution of the first destabilization times of Mercury.—We now discuss qualitatively the implications of the existence of a slow variable for Mercury's destabilization. This discussion is best understood looking at the level curves of $H_{\text{int}}(I, J)$ in action space displayed in Fig. 2. It can be seen that the landscape defined by $H_{\text{int}}(I, J)$ has the topology of a saddle. The saddle is exactly located at the intersection between the two resonances $g_1 - g_5$ and $s_1 - s_2$, with the value $H_{\text{int}} = H_{\text{cr}}$. The domain of equation $H_{\text{int}}(I, J) \geq H_{\text{cr}}$ has two disjoint components, one bounded (bottom left) and the other unbounded (top right), only connected by the saddle point $(I_{\text{cr}}, J_{\text{cr}})$. The initial orbital parameters of Mercury e and i are located in the bounded domain, which implies that the short-time orbital fluctuations are restricted to this part of phase space. When H_{int} reaches the value H_{cr}, Mercury can cross the saddle and enter the unbounded domain of phase space. This latter event defines Mercury's destabilization.

We explain in the Supplemental Material [29] how the above simple criterion translates into an equivalent criterion for $\tilde{H}'$: there exists a threshold h_{cr} for which the first destabilization time exactly corresponds to the first hitting time of $\tilde{H}'$ to h_{cr}.

The full expression of $\tilde{H}'$ is an intricate series composed of a large number of periodic terms of small amplitude, which explicit expression is difficult to handle. Following [26], we prefer to use in practice the local time average $h(t) = \langle \tilde{H} \rangle_{[t-\theta, t+\theta]}$ as an approximation of $\tilde{H}'$, which is much simpler to implement numerically. The time frame θ has to be much larger than the frequency of the fast variations of $\tilde{H}$ given by the frequency $g_2 - g_5$ according to Eq. (5). As an example, the time variations of $\tilde{H}(t)$ compared to those of $h(t)$ is displayed in Fig. 3 with $\theta = 2$ Myr. We then identify the diffusion Eq. (8) for $\tilde{H}'$ and that for h.

Tracking numerically the value of $h(t)$ of trajectories leading to destabilization confirms that the distribution $h(\tau)$ (where τ is the destabilization time) is peaked at the value $h_{\text{cr}} = -0.048$, which can thus be identified as the destabilization threshold. We must also add a reflective boundary for a upper value h_{sup}, accounting for the fact that the chaotic region of phase space before destabilization is
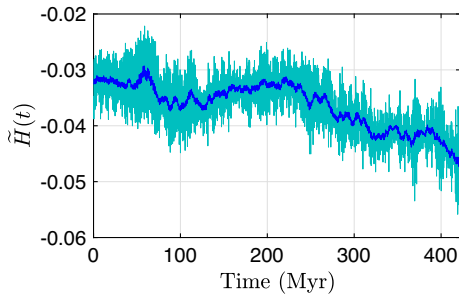
FIG. 3. A trajectory $\tilde{H}(t)$ (cyan) compared to its local time average $h(t)$ (blue). The local time averaging of $\tilde{H}(t)$ suppresses the fast oscillations that do not correspond to long-term variations. For the long-term chaotic dynamics, $h(t)$ is an slow variable that follows a standard Brownian motion.

bounded. Destabilization of Mercury occurs when the Brownian motion defined by $h(t)$ reaches h_{cr}. For a standard Brownian motion, the distribution $\rho(\tau)$ of first hitting times of the value h_{cr} can be derived exactly (see [29]). The latter is displayed in Fig. 4, together with the distribution obtained from direct numerical simulations of Hamilton's equations. D is the only fitting parameter and can be estimated as $D \approx 9.6 \times 10^{-7}$ Myr^{-3}. Using this value, Fig. 4 shows that the diffusive model Eq. (8) gives a excellent qualitative agreement with the direct numerical simulations. The fitted value of D is also in agreement with Eq. (9) and its order of magnitude $D \approx 7.2 \times 10^{-7}$ Myr^{-3}.

Instanton paths for Mercury.—We now focus on the probability that Mercury's orbit is destabilized in short times $\tau_L \ll \tau \ll \tau^*$, where τ^* is the maximum of $\rho(\tau)$. The probability $\mathbb{P}(\tau) = \int_0^\tau \rho_{\mathrm{th}}(\tau') d\tau'$ that the destabilization of Mercury's orbit occurs in a time shorter than τ is dominated at short times by the exponential term $\rho(\tau) \underset{\tau \to 0}{\asymp} e^{-(\bar{\tau}/\tau)}$, where $\bar{\tau} = \{[(h_0 - h_{\mathrm{cr}})^2]/4D\} \approx 1.56 \times 10^9$ years.

The exponential growth is the signature that short-term destabilizations of Mercury are rare events. The slow variable $h(t)$, conditioned on the fact that destabilization occurs at a given time τ, is predictable by the instanton path. The dynamics of $h(t)$ is simple enough such that the
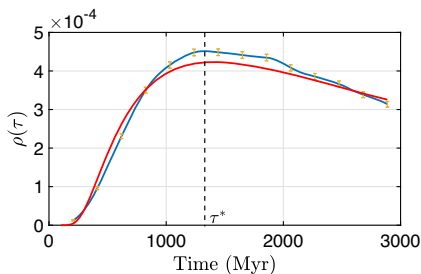
instanton path can be computed exactly: it is the straight path starting at $h(0)$ and reaching h_{cr} at time τ. We can even obtain a more precise result, namely the exact expressions for the average and the variance of all trajectories destabilized in a given time τ. The theoretical and numerical results for $\tau = 445$ million years is displayed in Fig. 5. The middle blue curve displays the averaged trajectory obtained through direct numerical averaging of all trajectories leading to destabilization at time τ. In addition, the upper and lower blue curves display the variance of the trajectories ensemble, and show how the trajectories depart from the most probable trajectory. We have superimposed three red curves that represent the average and variance of the probability distribution $\mathbf{P}[h, t|(h_{\mathrm{cr}}, \tau), (h_0, 0)]$ to observe the value h at time t, with the constrain $h(\tau) = h_{\mathrm{cr}}$, for the standard Brownian motion $h(t)$.

The agreement between the diffusive model of h and Mercury's dynamics can be considered as excellent, notwithstanding the small discrepancy at short times coming from the finite correlation time of Mercury's secular dynamics. This is a second confirmation that the diffusive model for the slow variable is consistent both for the prediction of Mercury's first destabilization time distribution, and for the prediction of instantons. However, we note that the simple picture of a straight-line instanton is bound to the validity of the diffusive limit used to derive Eq. (8). The simple approach described in this Letter would fail if, for example, the averaged dynamics of $\tilde{H}'$ would not be negligible.

Within the Batygin-Morbidelli-Holman dynamics, a reduced model of the inner Solar System with deterministic chaos, we have shown that the first exit time for a Mercury-Jupiter resonance can be computed from an effective stochastic diffusion. We have gone beyond this result, and we predicted the related instanton and demonstrated that path probabilities actually concentrate close to this instanton, for events which occur within a few hundred million years. For the Batygin-Morbidelli-Holman model,
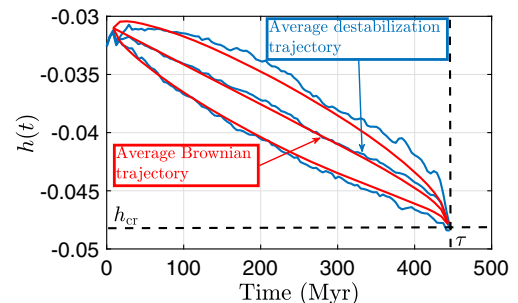
FIG. 5. Prediction of the trajectory leading to Mercury's short-term destabilization. The blue curves display the average trajectory and the variance of the trajectories leading to a destabilization at $\tau = 445$ million years, obtained with direct numerical simulations. The red curves display the same quantities obtained with the theory of rare events (prediction of the instanton, see [29]).

FIG. 4. Probability distribution of Mercury's first destabilization time. The distribution of Mercury's first destabilization time is computed with a direct numerical simulation (blue curve) and with the theoretical prediction of the diffusive model Eq. (8) (red curve).

both the instanton and the variance of the trajectories leading to Mercury's destabilization can be computed exactly. While the model contains some of the features of the inner Solar System dynamics, it neglects others. Clearly, this model should not be expected to quantitatively predict first exit times for the actual Solar System. Nevertheless, the instanton phenomenology is robust to more complex dynamics. Even if the secular dynamics of the real Mercury cannot be reduced to a simple diffusion model as done in this Letter, our striking results suggest that the destabilization of the Solar System might indeed occur though an instanton phenomenology. Our work opens this question: it should be addressed within other models, which have to be realistic enough for describing faithfully the actual dynamical mechanisms, but simple enough for a proper statistical study.

[1] F. Ragone, J. Wouters, and F. Bouchet, Computation of extreme heat waves in climate models using a large deviation algorithm, Proc. Natl. Acad. Sci. U.S.A. 115, 24 (2018).

[2] J. S. Langer, Theory of the condensation point, Ann. Phys. (N.Y.) 41, 108 (1967).

[3] S. R. Coleman, The uses of instantons, Subnuclear series 15, 805 (1979).

[4] J. Zinn-Justin, Quantum Field Theory and Critical Phenomena (Clarendon Press, Oxford, 1996).

[5] J. S. Langer, Excitation Chains at the Glass Transition, Phys. Rev. Lett. 97, 115704 (2006).

[6] N. G. van Kampen, Stochastic Processes in Physics and Chemistry, North-Holland Personal Library, 3rd ed. (Elsevier, Amsterdam, Boston, 2007).

[7] E. Woillez, Y. Zhao, Y. Kafri, V. Lecomte, and J. Tailleur, Activated Escape of a Self-Propelled Particle from a Metastable State, Phys. Rev. Lett. 122, 258001 (2019).

[8] M. Berhanu, R. Monchaux, S. Fauve, N. Mordant, F. Petrelis, A. Chiffaudel, F. Daviaud, B. Dubrulle, L. Marie, F. Ravelet, M. Bourgoin, P. Odier, J. Pinton, and R. Volk, Magnetic field reversals in an experimental turbulent dynamo, Eur. Phys. Lett. 77, 59001 (2007).

[9] T. Grafke, R. Grauer, and T. Schäfer, Instanton filtering for the stochastic Burgers equation, J. Phys. A 46, 062002 (2013).

[10] J. Laurie and F. Bouchet, Computation of rare transitions in the barotropic quasi-geostrophic equations, New J. Phys. 17, 015009 (2015).

[11] T. Grafke, R. Grauer, and S. Schindel, Efficient computation of instantons for multi-dimensional turbulent flows with large scale forcing, Commun. Comput. Phys. 18, 577 (2015).

[12] F. Bouchet, J. Rolland, and E. Simonnet, Rare Event Algorithm Links Transitions in Turbulent Flows with Activated Nucleations, Phys. Rev. Lett. 122, 074502 (2019).

[13] G. Dematteis, T. Grafke, and E. Vanden-Eijnden, Rogue waves and large deviations in deep sea, Proc. Natl. Acad. Sci. U.S.A. 115, 855 (2018).

[14] T. Grafke and E. Vanden-Eijnden, Numerical computation of rare events via large deviation theory, Chaos 29, 063118 (2019).

[15] M. I. Freidlin and A. D. Wentzell, Random Perturbations of Dynamical Systems, 3rd ed. (Springer-Verlag, New York, 2012).

[16] R. Graham, Macroscopic potentials, bifurcations and noise in dissipative systems, in Fluctuations and Stochastic Phenomena in Condensed Matter, edited by L. Garrido, Lecture Notes in Physics Vol. 268 (Springer, Berlin, Heidelberg, 1987).

[17] Please note that the word "action" refers to the path integral of large deviation theory, and has nothing to do with the classical action of analytical mechanics that can be written for Hamiltonian dynamics.

[18] J. Laskar, A numerical experiment on the chaotic behaviour of the solar system, Nature (London) 338, 237 (1989).

[19] J. Laskar, The chaotic motion of the solar system: A numerical estimate of the size of the chaotic zones, Icarus 88, 266 (1990).

[20] G. J. Sussman and J. Wisdom, Chaotic evolution of the solar system, Science 257, 56 (1992).

[21] J. Laskar and M. Gastineau, Existence of collisional trajectories of mercury, mars and venus with the Earth, Nature (London) 459, 817 (2009).

[22] K. Batygin and G. Laughlin, On the dynamical stability of the solar system, Astrophys. J. 683, 1207 (2008).

[23] J. Laskar, Chaotic diffusion in the Solar System, Icarus 196, 1 (2008).

[24] G. Boué, J. Laskar, and F. Farago, A simple model of the chaotic eccentricity of mercury, Astron. Astrophys. 548, A43 (2012).

[25] E. Woillez and F. Bouchet, Long-term influence of asteroids on planet longitudes and chaotic dynamics of the solar system, Astron. Astrophys. 607, A62 (2017).

[26] K. Batygin, A. Morbidelli, and M. J. Holman, Chaotic disintegration of the inner Solar System, Astrophys. J. 799, 120 (2015).

[27] J. Laskar and P. Robutel, Stability of the planetary three-body problem, Celest. Mech. Dyn. Astron. 62, 193 (1995).

[28] Y. Lithwick and Y. Wu, Theory of secular chaos and Mercury's orbit, Astrophys. J. 739, 31 (2011).

[29] See the Supplemental Material at http://link.aps.org/supplemental/10.1103/PhysRevLett.125.021101 for the values of coefficients in Eqs. (2) and (3), the list of third order resonances in Eq. (6), details about the derivation of Eq. (9), the critical threshold for the slow variable, and the explicit expression for the distribution of first exit time of a Brownian motion from a bounded domain, which includes Refs. [30,31].

[30] A. Morbidelli and A. Giorgilli, On the role of high order resonances in normal forms and in separatrix splitting, Physica (Amsterdam) **102D**, 195 (1997).

[31] G. Li and K. Batygin, On the spin-axis dynamics of a moonless Earth, Astrophys. J. **790**, 69 (2014).

[32] This value is actually specific of our model. The current value of g_1 for the real Solar System would be about $5.60''/$yr.

[33] J. Laskar, Frequency analysis for multi-dimensional systems. Global dynamics and diffusion, Physica (Amsterdam) **67D**, 257 (1993).

[34] A. Morbidelli, *Modern Celestial Mechanics: Aspects of Solar System Dynamics* (Taylor & Francis, London, 2002).

[35] TRIP is a general computer algebra system dedicated to celestial mechanics developed at the IMCCE (Copyright 1988-2019, J. Laskar ASD/IMCCE/CNRS). TRIP is particularly efficient to handle series with a large number of terms like those usually appearing in Lie transforms.

[36] C. W. Gardiner, *Stochastic Methods* (Springer-Verlag, Berlin, Heidelberg, New York, Tokyo, 1985).